Int. J. Solids Structures Vol. 30, No. 12, pp. 1579–1587, 1993
Printed in Great Britain

0020–7683/93 $6.00+ .00
Pergamon Press Ltd

NONDESTRUCTIVE CAVITY IDENTIFICATION IN STRUCTURES

SHUN-CHIEH HSIEH and TOSHIO MURA
Department of Civil Engineering, The Technological Institute, Northwestern University, 2145 Sheridan Road, Evanston, IL 60208, U.S.A.

(*Received* 21 *July* 1992; *in revised form* 27 *December* 1992)

Abstract—An algorithm for solving an inverse problem in elastostatics is developed. In this problem, the location and shape of the cavity are unknown. Instead, extra experimental data are provided at several internal points in the structure. Through an iterative process, the unknown boundary is determined by using the boundary element method coupled with nonlinear optimization technique. Some illustrated numerical examples are presented to demonstrate the method. Through these examples the effects of the error in the internal displacement data and of the number of measurement points and their locations are examined.

1. INTRODUCTION

The definition of an *inverse problem* is described by Tikhonov and Arsenin (1977) as follows. Formally, to solve an inverse problem means to discover the cause of a known result. Hence, all problems of the interpretation of observed data are actually inverse. Inverse problems in solid mechanics arise when insufficient boundary conditions are prescribed, but additional information on the solution, such as displacements or strains at specified internal points in the body, is given. These measurements are often performed at internal points in the body due, for example, to difficulties in placing sensors on boundaries where the specimen is in contact with another body. Inverse problems bring together the best features of both analysis and testing. Ideally, using known test data and approaching the problem inversely can result in the actual determination of boundary conditions.

Inverse deformation problems have been discussed in the field of structural dynamics by Trujillo (1978), thermoelasticity by Grysa *et al.* (1981), vibration problems by Gladwell (1986), nondestructive measurement of plastic strains by Mura *et al.* (1986), and over-prescribed elastostatics by Maniatty *et al.* (1989) and by Yeih *et al.* (1992). An overview of the inverse problems arising in the fields of mechanics and fracture of solids and structures is presented by Kubo (1988).

In recent years, the main emphasis of inverse problems has been concentrated in the area of nondestructive inspection involved in finding flaws or defects included in structural components. The uniqueness of the solution has been established by Ramm (1986), Friedman and Vogelius (1989), and Kubo *et al.* (1989). *Inverse shape determination problem* has been performed by Tanaka and Masuda (1986). In this reference, a Taylor series expansion of the boundary integral equation is used to obtain the unknown boundary by distorting a guessed boundary in an iterative process. Internal stresses are used as reference data which are obtaind by experiment. This method requires a large number of data points and additional care in evaluating singular integrals which appear due to the differentiation in the Taylor expansion. Murai and Kagawa (1986) employ boundary element iterative techniques by using boundary impedance as reference data to determine interface boundary between two domains with different conductivity for application to impedance plethysmography. In the above papers, there are no discussions about the stability of solutions. Nishimura and Kobayashi (1991) apply the boundary element method in crack identification by using boundary measurement of displacements and slopes. However, it has been shown to require solutions of certain hypersingular integral equations in the process of minimization. Special regularization techniques which are different from Tikhonov's regularization method are proposed to solve these integral equations. Das (1991) develops an algorithm for the flaw identification problem in steady-state heat conduction by using boundary temperatures as reference data. This method does not involve evaluation of singular integrals. However, the method requires a large number of iterations and does not tolerate experimental errors. This deficiency makes it impossible for practical application since the real experimental data usually contain some amount of unspecified measurement errors. Dulikravich and Kosovic (1992) use boundary element method and Davidon–Fletcher–Powell optimization for void identification in heat conduction problem. But two types of extra data must be specified, i.e. surface temperatures and heat fluxes.

Nondestructive cavity identification is one of the most important issues in evaluating structural safety and life-time of operating plants and structures. Various nondestructive examination methods for cavity detection have been researched and developed so far. Nevertheless, much work is still required in improving accuracy and efficiency for further practical application. The present paper will start with the precise definition of the cavity identification problem in elastostatics. Then, the nonlinear optimization technique used for the solution will be presented along with specific numerical examples examining the effect of the error in the measurement data as well as of the number and position of the measure points.

2. STATEMENT OF THE PROBLEM

Consider a plate D as shown in Fig. 1. It is assumed that the material properties of the plate are homogeneous, isotropic and linearly elastic. Some parts of the boundary, $|D|_t$, are traction prescribed and the rest, $|D|_u$, are displacement prescribed. Also consider that the displacements are obtained experimentally at several selected internal points. If the plate contains a cavity Ω, the measured displacements will be different from those for a plate without a cavity. Conversely, this difference in displacement indicates the presence of the cavity. Further, one can use the prescribed displacement and traction conditions on $|D|_u+|D|_t$ and the additional experimental information, and attempt to determine the location and shape of the cavity.

The displacements at some internal points indicated by the dots in Fig. 1 can be obtained numerically by the boundary element method, and also experimentally, for example, by the Moiré method. Ideally, the values obtained by these two methods should match within certain acceptable limits. However, the boundary element method does not give correct values of the displacements at the internal points when there is a cavity at an unknown location, of unknown shape and of unknown size. Because the boundary element

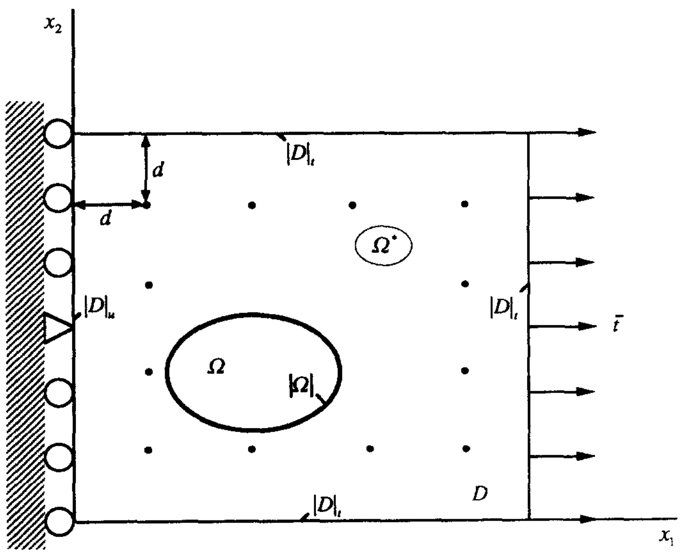

Fig. 1. Plate with an elliptical cavity. Thick solid curve—real cavity, thin solid curve—guessed cavity, dots—sensors.

method needs the correct boundaries of D and the boundary values of displacement and traction. In this paper we have assumed that there could only be one cavity Ω with traction-free boundary $|\Omega|$ in the plate. Our aim is to determine $|\Omega|$ from the measured displacement data at some selected points. The scheme for solving this inverse problem is described in the following section.

3. BOUNDARY ELEMENT METHOD AND NONLINEAR OPTIMIZATION TECHNIQUE

The differential equation which governs linear elastostatics without body forces is

$$C_{kjmn}u_{m,nj} = 0, \quad \text{in } D, \tag{1}$$

where C_{kjmn} are the elastic moduli and u_m is the displacement. Equation (1) must be accompanied by boundary conditions

$$\begin{aligned} t_k &= C_{kjmn}u_{m,n}n_j = \bar{t}_k, \quad \text{on } |D|_t, \\ u_k &= 0, \quad \text{on } |D|_u, \\ t_k &= 0, \quad \text{on } |\Omega|, \end{aligned} \tag{2}$$

where t_k is the traction, n_j is the outward-pointing normal vector and $\bar{t}_k$ is the prescribed value for traction. The differential equation can be converted into the boundary integral equation (Kinoshita and Mura, 1956; Kitahara, 1985),

$$c_{lk}u_k(\mathbf{x}') = \int_{|D|} [G_{lk}(\mathbf{x},\mathbf{x}')t_k(\mathbf{x}) - H_{lk}(\mathbf{x},\mathbf{x}')u_k(\mathbf{x})]\,\mathrm{d}s(\mathbf{x}), \tag{3}$$

which gives the value of displacement at any point $\mathbf{x}'$ when the boundary values of displacement and traction on $|D| = |D|_t + |D|_u + |\Omega|$ are given. The coefficient c_{lk} is given as

$$\begin{aligned} c_{lk} &= 0, && \text{if } \mathbf{x}' \text{ lies outside } D+|D|, \\ c_{lk} &= 1, && \text{if } \mathbf{x}' \text{ lies inside } D, \\ c_{lk} &= \tfrac{1}{2}\delta_{lk}, && \text{if } \mathbf{x}' \text{ lies on } |D|, \end{aligned} \tag{4}$$

where $|D|$ is smooth at $\mathbf{x}'$. δ_{lk} is the Kronecker symbol. The two-point functions $G_{lk}(\mathbf{x},\mathbf{x}')$ and $H_{lk}(\mathbf{x},\mathbf{x}')$ are displacement and traction components of the Kelvin's fundamental solutions for the plane strain problems displayed as follows:

$$G_{lk}(\mathbf{x},\mathbf{x}') = \frac{1}{8\pi\mu(1-\nu)}\left[-(3-4\nu)\delta_{lk}\ln R_1 + \frac{(x_l-x_l')(x_k-x_k')}{R_1^2}\right], \tag{5}$$

$$H_{lk}(\mathbf{x},\mathbf{x}') = \frac{1}{4\pi(1-\nu)}\left\{-\left[\frac{1-2\nu}{R_1}\delta_{lk} + \frac{2(x_l-x_l')(x_k-x_k')}{R_1^3}\right]\frac{\partial R_1}{\partial n} + (1-2\nu)\left[\frac{x_l-x_l'}{R_1^2}n_k - \frac{x_k-x_k'}{R_1^2}n_l\right]\right\}, \tag{6}$$

where

$$R_1^2 = (x_1-x_1')^2 + (x_2-x_2')^2,$$

n_l and n_k are the direction cosines of the normal with respect to x_l and x_k. Plane stress problems can be solved by using the equivalent Poisson's ratio $\nu' = \nu/(1+\nu)$. The value of the shear modulus μ remains the same. Substituting the boundary conditions (2), we write eqn (3) as

$$c_{lk}u_k(\mathbf{x}') = \int_{|D|_t} [G_{lk}(\mathbf{x},\mathbf{x}')\bar{t}_k(\mathbf{x}) - H_{lk}(\mathbf{x},\mathbf{x}')u_k(\mathbf{x})]\,\mathrm{d}s(\mathbf{x}) + \int_{|D|_u} [G_{lk}(\mathbf{x},\mathbf{x}')t_k(\mathbf{x})]\,\mathrm{d}s(\mathbf{x}) - \int_{|\Omega|} [H_{lk}(\mathbf{x},\mathbf{x}')u_k(\mathbf{x})]\,\mathrm{d}s(\mathbf{x}). \quad (7)$$

The first step of the computational scheme is to assume a cavity boundary $|\Omega^*|$. Then (7) is written as

$$c_{lk}u_k^*(\mathbf{x}') = \int_{|D|_t} [G_{lk}(\mathbf{x},\mathbf{x}')\bar{t}_k(\mathbf{x}) - H_{lk}(\mathbf{x},\mathbf{x}')u_k^*(\mathbf{x})]\,\mathrm{d}s(\mathbf{x}) + \int_{|D|_u} [G_{lk}(\mathbf{x},\mathbf{x}')t_k^*(\mathbf{x})]\,\mathrm{d}s(\mathbf{x}) - \int_{|\Omega^*|} [H_{lk}(\mathbf{x},\mathbf{x}')u_k^*(\mathbf{x})]\,\mathrm{d}s(\mathbf{x}), \quad (8)$$

where u_k^* and t_k^* are u_k and t_k when $|\Omega|$ is assumed to be $|\Omega^*|$. These values depend not only on $\mathbf{x}'$ but also on the choice of parameter $\mathbf{z}$ describing $|\Omega^*|$. Let

$$F_l^*(\mathbf{x}',\mathbf{z}) = u_l^*(\mathbf{x}'), \quad (9)$$

where $\mathbf{x}'$ are point vectors of M number of selected points inside D and $\mathbf{z}$ is a vector with N components, which defines $|\Omega^*|$. The objective is to fit the mathematical function $F_l^*(\mathbf{x}',\mathbf{z})$ to the experimental data $u_l(\mathbf{x}')$ by varying $\mathbf{z}$. When $F_l^*(\mathbf{x}',\mathbf{z})$ is nonlinear in $\mathbf{z}$ which is the variable of the optimization problem, this type of problem is called *nonlinear regression*. Generally $2M > N$ and the system is then said to be *overdetermined*; the case $2M < N$ characterizes an *underdetermined* system.

It is necessary to define more precisely what we mean by the best fit. For most overdetermined systems it will not be possible to find $\mathbf{z}$ such that $F_l^*(\mathbf{x}',\mathbf{z})$ matches the experimental data at all points. The difference between $u_l(\mathbf{x}')$ and $F_l^*(\mathbf{x}',\mathbf{z})$ is called a *residual* r_l,

$$r_l^m(\mathbf{z}) = F_l^*(\mathbf{x}'^{(m)},\mathbf{z}) - u_l(\mathbf{x}'^{(m)}), \quad l = 1,2, \quad m = 1,\ldots,M. \quad (10)$$

Finally, the *least squares best fit* is obtained by minimizing the function which is the sum of the squares of the residuals

$$\sum_{m=1}^{M} [r_l^m(\mathbf{z})]^2, \quad l = 1,2, \quad (11)$$

with respect to $\mathbf{z}$. Squares are taken to avoid cancellation between residuals of opposite sign. The residuals are nonlinear functions of $\mathbf{z}$, therefore this is a *nonlinear least squares problem*. Altogether, one can evaluate $2M$ quantities (r_l^m, $l = 1,2$; $m = 1,2,\ldots,M$) for the M number of selected points. During the minimization process, the quantity $|\Omega^*|$ is modified, and at the conclusion of the process $|\Omega^*|$ converges to $|\Omega|$. The details of the algorithm for updating the unknowns at the end of each cycle are presented as follows.

The real unknown cavity, $|\Omega|$, could be of any general shape. However, in this demonstrative scheme, all cavities are assumed to be elliptical to reduce the degrees of freedom (DOF) and computation time. Moreover, the elliptical shape covers a wide range of shapes from circular holes to straight cracks. Instead of considering the coordinates of the end points of elements as the unknowns, the location of the center (z_1, z_2), the semi-major axis z_3, the semi-minor axix z_4 and the angular orientation z_5 of the semi-major axis with the x_1-axis are considered as the ultimate unknowns of the problem (DOF = 5).

The nonlinear least squares problem is stated as follows:

$$\text{Given}\quad \mathbf{R}:\mathbb{R}^N \to \mathbb{R}^M,\quad M \geqslant N,$$
$$\text{find}\quad \mathbf{z}\in\mathbb{R}^N \quad \text{for which}\quad \sum_{m=1}^{M} [r^m(\mathbf{z})]^2 \quad \text{is minimized,} \tag{12}$$

where $\mathbf{R} = \mathbf{R}_1$ or $\mathbf{R}_2$, $r = r_1$ or r_2, $\mathbb{R}^N$ denotes N-dimensional Euclidean space and $r^m(\mathbf{z})$ is the mth component of $\mathbf{R}(\mathbf{z})$. Let's define the *Jacobian* and *Hessian* of $\mathbf{R}$ at $\mathbf{z}$ before we try to solve problem (12).

Definition. A continuous function $\mathbf{R}:\mathbb{R}^N \to \mathbb{R}^M$ is continuously differentiable at $\mathbf{z}\in\mathbb{R}^N$ if each component function R_i, $i = 1,\ldots,M$ is continuously differentiable at $\mathbf{z}$. The derivative of $\mathbf{R}$ at $\mathbf{z}$ is called the Jacobian (matrix) of $\mathbf{R}$ at $\mathbf{z}$, and its transpose is called the gradient of $\mathbf{R}$ at $\mathbf{z}$. If the N^2 second partial derivatives of $\mathbf{R}$ also exist and are continuous, the matrix containing them is called the Hessian of $\mathbf{R}$ at $\mathbf{z}$. The common notations are:

$$\mathbf{J}(\mathbf{z}) = \frac{\partial \mathbf{R}(\mathbf{z})}{\partial \mathbf{z}} = [\nabla \mathbf{R}(\mathbf{z})]^{\mathrm{T}}, \tag{13}$$

$$\mathbf{H}(\mathbf{z}) = \nabla^2 \mathbf{R}(\mathbf{z}) = [\mathbf{J}(\mathbf{z})]^{\mathrm{T}}\mathbf{J}(\mathbf{z}). \tag{14}$$

Now suppose that we have $\mathbf{z}_c$ which corresponds to initial guess and some estimate $\boldsymbol{\delta}_c$ of the maximum length of a successful step we are likely to be able to take from $\mathbf{z}_c$. The step $\Delta\mathbf{z}$ that solves

$$\min_{\Delta\mathbf{z}\in\mathbb{R}^N} \mathbf{R}(\mathbf{z}_c+\Delta\mathbf{z}) = \|\mathbf{R}(\mathbf{z}_c)+\mathbf{J}(\mathbf{z}_c)\Delta\mathbf{z}\|_2$$
$$\text{subject to}\quad \|\Delta\mathbf{z}\|_2 \leqslant \delta_c, \tag{15}$$

is the best step of maximum length δ_c from $\mathbf{z}_c$. $\|\cdot\|_2$ designates the l_2 norm. Problem (15) is the basis of the *model-trust region* approach to minimization. Its solution is given in the following lemma. The name comes from viewing δ_c as providing a *region* in which we can *trust* $\mathbf{R}(\mathbf{z}_c+\Delta\mathbf{z})$ to adequately *model* $\mathbf{R}(\mathbf{z}_c)$.

Lemma. Let $\mathbf{R}:\mathbb{R}^N \to \mathbb{R}^M$ be twice continuously differentiable, the Hessian of $\mathbf{R}$ at $\mathbf{z}_c$, $\mathbf{H}_c\in\mathbb{R}^{N\times N}$ be symmetric and positive definite, and let $\mathbf{I}$ be the unit matrix of order N. Then the solution to problem (15) is

$$\Delta\mathbf{z}(\mu_c) = -[\mathbf{H}_c+\mu_c\mathbf{I}]^{-1}\mathbf{J}_c^{\mathrm{T}}\mathbf{R}_c, \tag{16}$$

where $\mu_c = 0$ if $\delta_c \geqslant \|\mathbf{H}_c^{-1}\mathbf{J}_c^{\mathrm{T}}\mathbf{R}_c\|_2$ and $\mu_c > 0$ otherwise. $\mathbf{R}_c$, $\mathbf{J}_c$ and $\mathbf{H}_c$ are the function value, the Jacobian and the Hessian calculated at the current point $\mathbf{z}_c$, respectively.

The proof of the lemma is provided by Dennis and Schnabel (1983). Formula (16) was first suggested by Levenberg (1944) and Marquardt (1963) and is known as the *Levenberg–Marquardt* method. The implementation (16) as a trust region algorithm, where μ_c and δ_c are chosen by the techniques of the locally constrained optimal step and of updating the trust region, is due to Moré (1977). Numerical results illustrating the behavior of the algorithm are presented in the following section.

4. NUMERICAL EXAMPLES

The main jobs when solving an inverse problem are given as follows. These will be illustrated by numerical examples.

(i) Find out whether the chosen model $F_l^*(\mathbf{x}', \mathbf{z})$ is compatible with the experimental data $u_l(\mathbf{x}')$, i.e. find such a function which is characterized by a vector $\mathbf{z}$ that

$$F_l^*(\mathbf{x}', \mathbf{z}) - u_l(\mathbf{x}') \leqslant \delta_l, \tag{17}$$

under the natural condition that

$$\mathbf{z}^* \to \mathbf{z} \quad \text{as} \quad \delta_l \to 0, \tag{18}$$

where $\mathbf{z}^*$ is the approximate solution and δ_l is the accuracy of measurement.

(ii) Determine, if possible, the errors of the approximate solutions within the adopted model, i.e. estimate the difference between $\mathbf{z}^*$ and $\mathbf{z}$.

Consider a plate D as shown in Fig. 1 subject to a uniform tension $\bar{t} = 100$ MPa. The 2100×1100 mm plate is 10 mm thick, and it is made of aluminum with shear modulus $\mu = 26{,}520$ MPa and Poisson's ratio $v = 0.3$. The entire plate is modeled with 64 constant elements on outer boundary; 48 constant elements on the boundary of the internal cavity. In this section the results for elliptical and nonelliptical cavity problems are presented. Through these examples, the convergence properties of the computational scheme will be demonstrated.

Ideally one must obtain displacements at selected points from experiments, however, for want of any experimental data, the direct boundary element method solutions were used as input for the inverse algorithm.

Consider the problem of finding a 45°-inclined elliptical cavity with semi-major axis 200 mm and semi-minor axis 50 mm located at (650 mm, 450 mm). Computation begins with a guessed cavity Ω^*. It converges to the real cavity after 14 iterations by using 26 sensors. The convergent process is plotted in Fig. 2.

The stability of the solution for the proposed algorithm is examined as follows. The boundary element method solutions are used to generate the internal displacements of all the internal nodes. These displacements are multiplied by $(1 + e \times RAN)$, where e is percent error and RAN is a random variable on the interval $[-1, 1]$, to play the role of inexact experimental measurements. Different values of percent error are introduced into internal displacement data and the effect on the solution is observed. The results are plotted in Fig. 3. For this problem, the distance d of sensor from the boundary is 100 mm. It is of significance that the errors in shape parameters are linearly proportional to the error in the internal displacement input.

The effect of the distance d of sensor from the boundary is also observed when constant error is introduced into the internal displacements by multiplying them by $(1 + 0.02 \times RAN)$. The results are plotted in Fig. 4. It is also found that using more sensors has no effect on the solution. In effect, the number of internal points does not affect the solution much, as long as an underdetermined system does not occur. However, the arrangement of sensors has a significant effect on the solution. For this example, if half the sensors are placed on

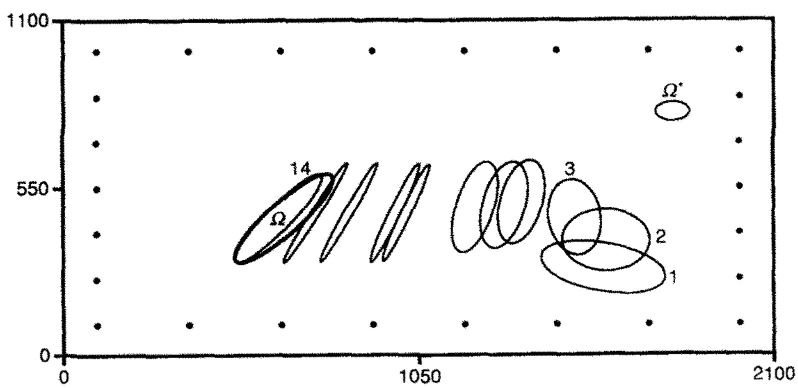

Fig. 2. Convergent process for elliptical cavity.

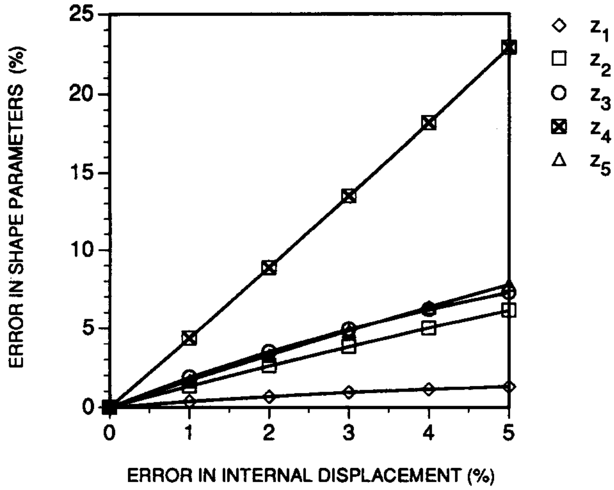

Fig. 3. Effect of error in internal displacement data.

the top and half on the bottom, the computation fails to converge. If half the sensors are placed on the right and half on the left, the number of iterations increases. Therefore, the optimum arrangement of sensors is to place them on four sides.

To demonstrate the superior performance of the scheme for a nonelliptical cavity, it is employed to find a 190 × 50 mm rectangular cavity with centroid at (675 mm, 495 mm). The algorithm provides a good estimate of the cavity as can be seen from Fig. 5. The example shows the robustness of the present approach.

5. CONCLUSIONS

A boundary element method formulation with a nonlinear least squares technique has been shown to be an effective and easy way for the inverse shape determination problems of elastostatics for which some experimental data are available. The calculation is initiated from an assumed cavity boundary until a real cavity boundary is achieved so as to match the displacements measured at some internal points of the plate. Even when one considers a nonelliptical cavity, one may still use the present approach of assuming the cavity to be elliptical. Indeed, such an analysis is expected to converge to a cavity sufficiently close to

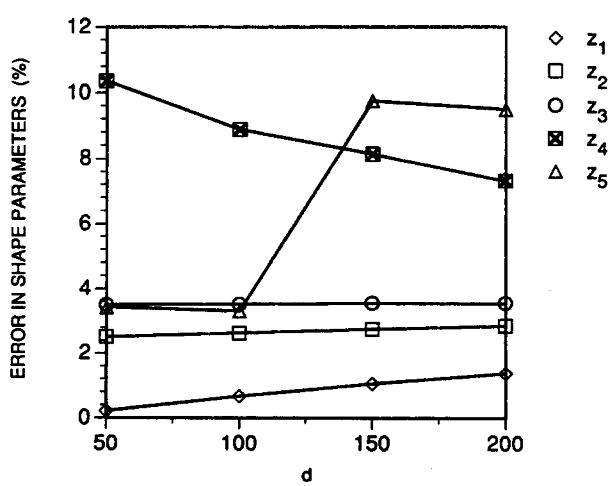

Fig. 4. Effect of distance of sensor from boundary with 2% random error in internal displacement input.

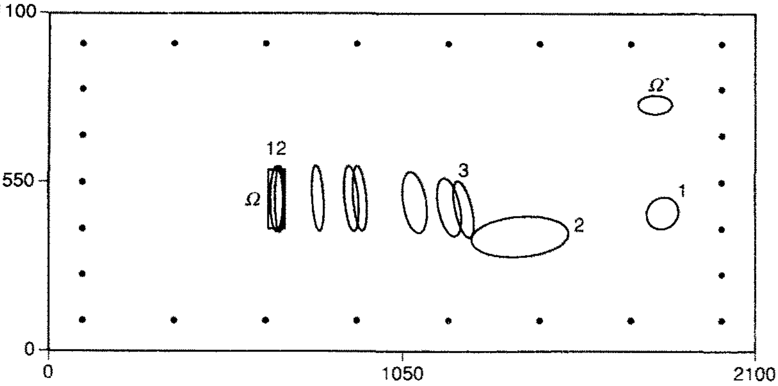

Fig. 5. Convergent process for rectangular cavity.

the true configuration. One may then use this cavity as a good, and therefore economical, initial guess in a more sophisticated inversion analysis which allows more degrees of freedom of the shape. The developed algorithm was found to be insensitive to the number of sensors. Further, the algorithm does not require additional care in evaluating singular integrals and can handle problems with measurement errors in input experimental data. These characteristics make this formulation more practical.

The application of the proposed method can be extended to scattering, heat conduction, and electromagnetic problems in three dimensions where the number of variables will be eight if the cavity is assumed to be an ellipsoid. For the extension to the three-dimensional problem, displacement data on the boundary should be used, since it is not possible to measure internal displacement in the three-dimensional problem.

Acknowledgements—This research was supported by the Air Force Office of Scientific Research under Grant No. AFOSR-F49620-92-J-0319 and partly by Amoco Production Company. The authors are pleased to acknowledge useful discussions with Dr Z. Moschovidis and Dr T. Koya.

REFERENCES

Das, S. (1991). Numerical solution of inverse problems in mechanics using the boundary element method. Ph.D. dissertation, Iowa State University, U.S.A.

Dennis, J. E. and Schnabel, R. B. (1983). *Numerical Methods for Unconstrained Optimization and Nonlinear Equations*. Prentice-Hall, Englewood Cliffs, NJ.

Dulikravich, G. and Kosovic, B. (1992). Determination of void shapes, sizes and locations inside an object with known surface temperatures and heat fluxes. In *Abstract of IUTAM Symposium on Inverse Problems in Engineering Mechanics*, Tokyo, Japan, 75–77.

Friedman, A. and Vogelius, M. (1989). Determining cracks by boundary measurements. *Indiana University Math. Jl* **38,** 527–556.

Gladwell, G. M. L. (1986). *Inverse Problems in Vibration*. Martinus Nijhoff, Dordrecht.

Grysa, K., Cialkowski, M. J. and Kaminski, H. (1981). An inverse temperature field problem of the theory of thermal stresses. *Nucl. Engng Design* **64,** 169–184.

Kinoshita, N. and Mura, T. (1956). On boundary value problem of elasticity. Research Reports of the Faculty of Engineering, Meiji University, No. 8, 56–82.

Kitahara, M. (1985). *Boundary Integral Equation Methods in Eigenvalue Problems of Elastodynamics and Thin Plates*. Elsevier, Amsterdam.

Kubo, S. (1988). Inverse problems related to the mechanics and fracture of solids and structures. *JSME International Journal, Series I* **31**(2), 157–166.

Kubo, S., Sakagami, T. and Ohji, K. (1989). On the uniqueness of the inverse solution in crack determination by the electric potential CT method (in Japanese). *Trans. Japan Soc. Mech. Engng* **55,** 2316–2319.

Levenberg, K. (1944). A method for the solution of certain nonlinear problems in least squares. *Q. Appl. Math.* **2,** 164–168.

Maniatty, A., Zabaras, N. and Stelson, K. (1989). Finite element analysis of some inverse elasticity problems. *J. Engng Mech.* **115**(6), 1303–1317.

Marquardt, D. W. (1963). An algorithm for least squares estimation for nonlinear parameters. *J. Soc. Indust. Appl. Math.* **11**(2), 431–441.

Moré, J. J. (1977). The Levenberg–Marquardt algorithm: implementation and theory. In *Numerical Analysis*, Lecture Notes in Math. 630 (Edited by G. A. Watson), pp. 105–116. Springer, Berlin.

Mura, T., Cox, B. and Gao, Z. (1986). Computer-aided nondestructive measurements of plastic strains from surface displacements. *Proc. Int. Conf. on Comput. Mech., Tokyo*, **2,** 43–48.

Murai, T. and Kagawa, Y. (1986). Boundary element iterative techniques for determining the interface boundary between two Laplace domains—a basic study of impedance plethysmography as an inverse problem. *Int. J. Numer. Meth. Engng* **23**, 35–47.

Nishimura, N. and Kobayashi, S. (1991). A boundary integral equation method for an inverse problem related to crack detection. *Int. J. Numer. Meth. Engng* **32**, 1371–1387.

Ramm, A. G. (1986). A geometrical inverse problem. *Inverse Problems* **2**, L19–L21.

Tanaka, M. and Masuda, Y. (1986). Boundary element method applied to some inverse problems. *Engng Anal.* **3**, 138–143.

Tikhonov, A. N. and Arsenin, V. Y. (1977). *Solution of Ill-posed Problems.* V. H. Winston and Sons, Washington, DC.

Trujillo, D. M. (1978). Application of dynamic programming to the general inverse problem. *Int. J. Numer. Meth. Engng* **12**, 613–624.

Yeih, W., Koya, T. and Mura, T. (1992). An inverse problem in elasticity with partially overprescribed boundary conditions, Part I: Theoretical Approach. *J. Appl. Mech.* (in press).